

THE DEGRADATION OF METAL SURFACES BY ATOMIC OXYGEN

A de Rooy

ESA/ESTEC Materials Section, Noordwijk, The Netherlands

ABSTRACT

The influence of atomic oxygen on the amount of erosion-corrosion of metal surfaces, especially silver, is examined. Protection schemes for silver are investigated. Bare silver samples and partly coated silver samples were exposed to low earth orbit conditions during Shuttle flights STS-8 and STS-17.

The silver specimens had decreased 3-4.5 μm in thickness depending on the relative position to the velocity vector. The examination of the coated silver samples shows that three coatings, namely 500nm palladium, 50 nm aluminium and the silicone DC6-1104 are successful in protecting the underlying silver against atomic oxygen attack.

Keywords: surfaces, SEM, Auger, atomic oxygen, oxidation, sputtering

1. INTRODUCTION

Atomic oxygen is one of the main constituents in the atmosphere at low earth orbit. The atomic oxygen oxidation of metals has been the topic of several studies. For the explanation of the mechanisms see ref. 1. Interaction of atomic oxygen with various surfaces like gold, stainless steel, titanium, carbon, osmium, teflon and pyrex were subject of previous investigations (ref. 2, 3, 4). The effect of atomic oxygen on surfaces in laboratory experiments (ref. 1, 2, 3) might be different from the effect encountered during low earth orbit (LEO) exposure, because far lower interaction

energies and no thermal cycling are used.

The relatively high capture efficiency for atomic oxygen of silver makes it a suitable detector for direct measurements in the upper atmosphere. These detectors depend on the formation of silver(II)-oxide and an increase in the resistance is observed. Although the formation of A90 is essential in this practise, its effect on silver when used for example as a structural or electrical item is undesirable, since it results in losses in both electrical conductivity and mechanical strength.

The major use of silver, exposed in the LEO environment, is as interconnector material in solar arrays. These interconnectors serve as the conductive path between cells forming the array.

As a result of the differences in thermal expansion coefficients of the several components of the solar array, high stresses are found in the interconnectors. If the performance of these interconnectors deteriorate by some action, loss of electrical power is observed.

In this investigation the effect of LEO exposure on silver was examined and several different coatings were applied to the silver to examine their protective effect, also an alternative interconnector material was tested.

The type of experiments and the method of examination are described in sections 2 and 3 respectively. The result of the optical, SEM, X-ray, Auger and microscopical examinations are presented in

section 4, and the overall results are discussed in section 5.

2. EXPERIMENTS

Four silver solar cell interconnectors (99.9% pure Ag foil, rolled then etched) were exposed to low earth orbit conditions in the cargo bay of shuttle flight STS-8. The interconnectors had been mounted on a supporting heaterplate maintained at 770C and exposed to atomic oxygen present in orbit between 300 and 1200 km.

Two samples were exposed perpendicular to the velocity vector, while the other two were exposed 45° to the velocity vector of the Space Shuttle (ref. 7)

Another twenty samples were exposed to LEO conditions during shuttle flight STS-17. To avoid possible contamination in the shuttle cargo bay these samples were mounted on the remote manipulator arm of the Space Shuttle.

Various schemes for the protection of the silver base metal were applied. Also two non-silver interconnect materials were tested, namely silver plated molybdenum and aluminium.

The sample types are presented in table I.

TABLE I

DESCRIPTION OF INTERCONNECT MATERIALS			
sample	type	protection	flight
1	Ag	none	STS-8
2	Ag	none	STS-8
3	Ag	50 nm Au	STS-17
4	Ag	500 nm Au	STS-17
5	Ag	500 nm Au*	STS-17
6	Ag	DC6-1104	STS-17
7	Ag	DC1200	STS-17
8	Mo	Ag/Pt	STS-17
9	Al	none	STS-17
10	Ag	50 nm Al	STS-17
11	Ag	50 nm Pd	STS-17
12	Ag	500 nm Pd	STS-17

The protection is normally applied via evaporation.

Sample 6 and 7 are protected with a silicone coating.

* = plated

3. EXAMINATION

The samples were examined optically before being cut into suitable strips for analysis by SEM, Auger and microsectioning.

Both front and back faces from sample 1 and 2 were examined in a JSM-T20 SEM and a JSM-T35 SEM fitted with a Link systems energy dispersive X-ray analyser and a four crystal wavelength dispersive X-ray spectrometer. Samples 3 to 12 were examined in a JSM-T300 SEM. Micrographs were taken and X-ray analysis performed. Sections of the interconnects were cut from the samples and mounted on submounts before examination in a Physical Electronics 590 Auger microscope equipped with two argon ion guns for depth profiling. Depth profiles were generated using an ion beam of 3 keV and $15 \mu\text{A}/\text{cm}^2$ current density (sample 1, 2 and 9 with $30 \mu\text{A}/\text{cm}^2$).

Microsections were made following standard procedures and diamond polished to $0.25 \mu\text{m}$. The microsections were examined on a Reichert MeF2 optical microscope.

4. RESULTS

4.1. Optical examination

Both front and back faces of the samples with exposed silver show brown-black stains except where they had been masked off by adhesive tape. On closer examina-

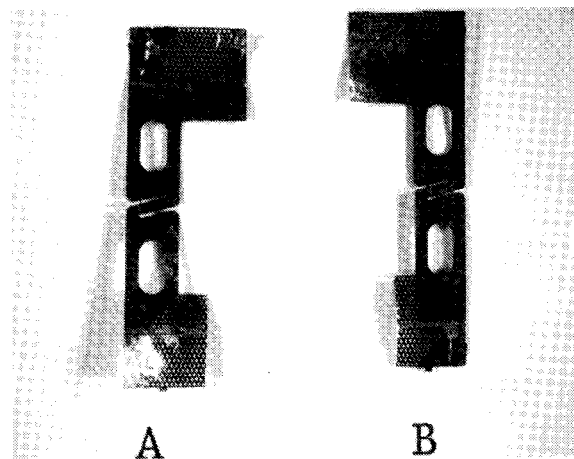


Figure 1. Macroview on the tested silver interconnectors. Note the discolouration on the surface. Magn. X 2.1.

tion the stains appear to be a thin scale which easily flakes away from the surface. (Fig. 1).

Two of the partly coated samples (3 and 7) exhibit changes in surfaces morphology. At higher magnification specimen 7 shows the same flakey appearance as the uncoated samples, while examination of specimen 3 reveals surface discolouration. The palladium coated samples revealed evidence of non-plated areas but these samples as well as the rest of the samples, are virtually unaffected by exposure to the LEO environment.

4.2. SEM examination and X-ray analysis

In all SEM pictures the flakey nature of the stains on the exposed silver is apparent and the underlying areas exposed by the flakes are visible. The thin flakes appears to be curling up and spalling away (fig. 2a). X-ray analysis indicates silver and chlorine associated with the stain. However, analyses of further stained areas reveal that the chlorine level associated with the stain is very variable and sometimes even nil. Wavelength dispersive X-ray analysis of the stained areas shows the presence of silver with low levels of oxygen and carbon with variable levels of chlorine.

Apart from the black shiny appearance of sample 3, the gold on the partly coated samples appears to be mainly unaffected (fig. 2b). The influence of the atomic oxygen on gold is evidenced by the difference in surface morphology of the 50 nm gold coating under the adhesive tape and the part exposed LEO. On the former region the black shiny appearance is absent. X-ray analysis records the presence of silver and sulphur on the 50 nm gold coating. X-ray analysis in the thicker 500 nm gold coatings reveal only sulphur being present.

The apparent atomic oxygen affect on the two silicone coatings differ considerable between each other. On the surface of the specimen coated with DC6-1104 (fig. 2c) no noticeable features are present, except for some charging effects due to the SEM environment, this is in contrast to the second silicone coating DC1200 "residue" (fig. 2d) where shiny and blackened areas are present.

This surface shows flakes curling up to expose underlying areas of bare silver.

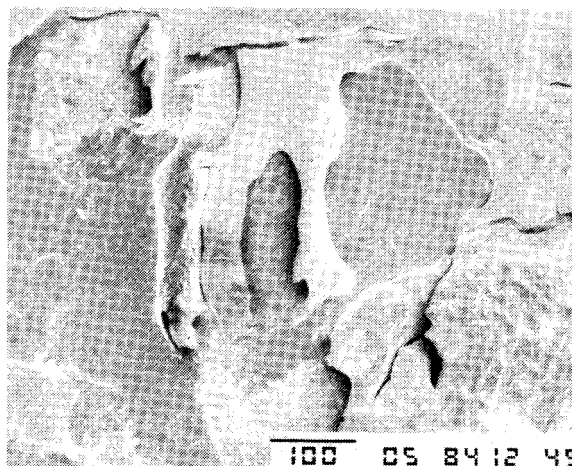


Figure 2a. Exposed silver surface. SEM micrograph showing flaking off of the silver-oxide layer. Notice a secondary flake (arrow) on an already attacked surface. Magn. X 150.

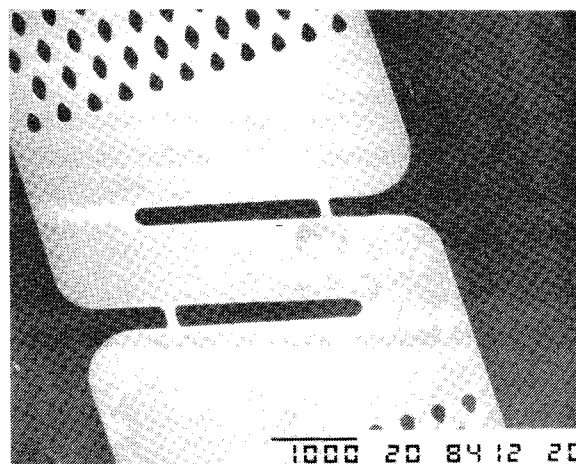


Figure 2b. Exposed partly coated silver surface (50 nm gold at arrow). SEM picture showing apparently no attack of the gold. Visual inspection revealed some discolouration of the gold. Magn. X 15.

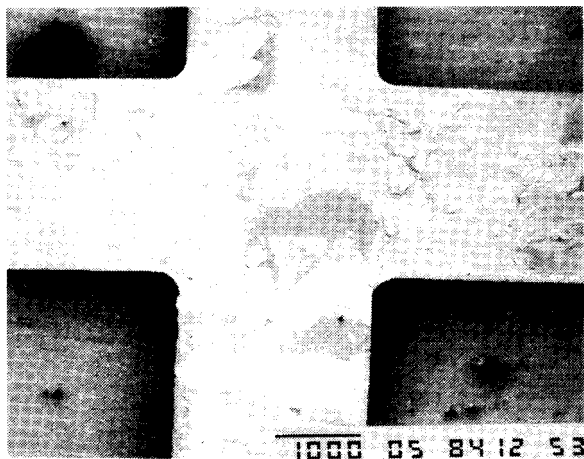


Figure 2e. Exposed silver coated molybdenum interconnector. SEM micrograph showing silver oxides flaking off of the surface. Molybdenum is not yet exposed. Magn. X 15.

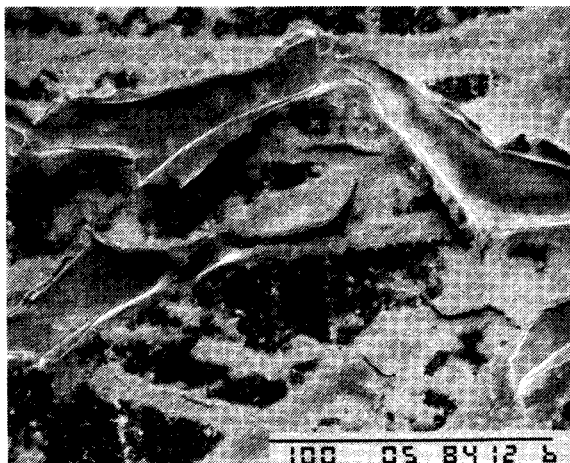


Figure 2d. Exposed silver foil coated with silicone DC1200 "residue". The SEM micrograph reveals silver-oxide flaking off of the surface, indicating that this coating is not protective. Magn. X 50.

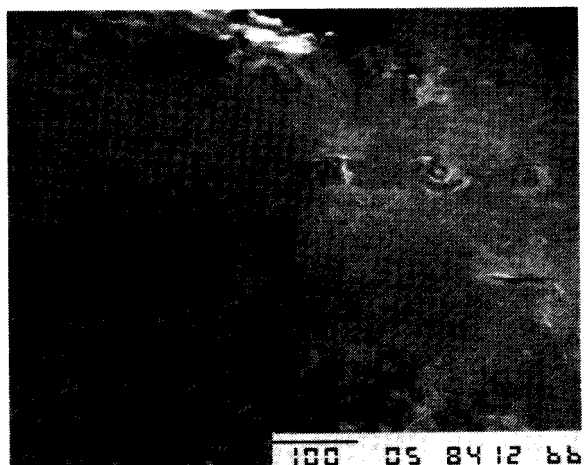


Figure 2c. Exposed silver foil coated with silicone DC6-1104. The SEM micrograph shows no signs of silver attack. Some charging due to the SEM environment is visible. Magn. X 150

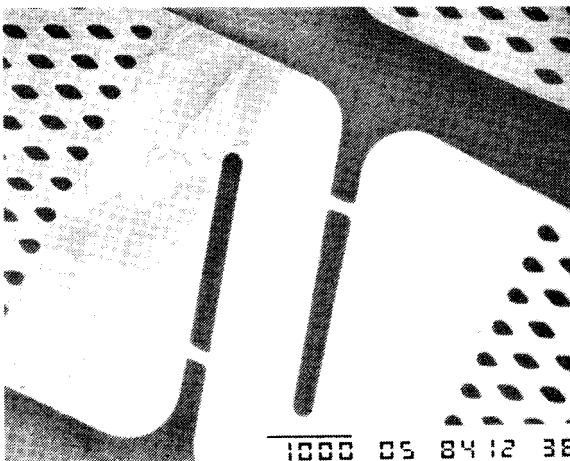


Figure 2f. Exposed partly coated silver interconnector (coating: 50 nm Al). No visible signs of attack are found on the aluminium surface. Magn. X 15.

Another widely used interconnector material in space technology is 5 μm silver coated molybdenum. After exposure to atomic oxygen the silver is flaking away as expected from the surface exposing underlying areas which have an etched appearance. This specimen was silver coated over the complete surface and consequently no bare molybdenum was exposed to LEO (fig. 2e). X-ray analysis reveals the presence of silver and traces of molybdenum and platinum.

One of the well known properties of aluminium is its very stable oxide in oxidising media. The two aluminium samples (one bare aluminium foil and one 50 nm aluminium coating on silver) illustrate this again. On the level of investigation in the SEM no affect of the atomic oxygen environment is encountered on these surfaces (fig. 2f).

Of the metals of the platinum group, palladium has promising properties in relation to atomic oxygen attack. No signs of flaking of the palladium are observed on both palladium coated silver interconnectors (fig. 2g).

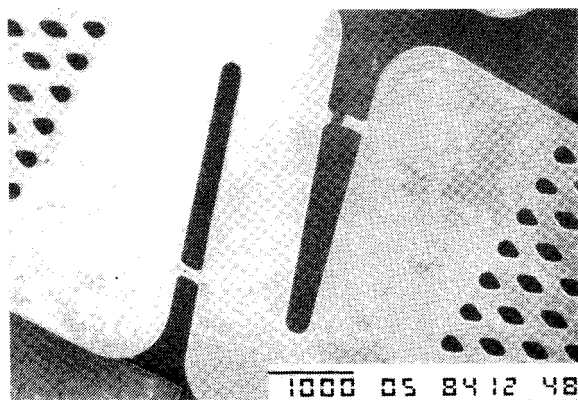


Figure 2g. Exposed partly coated silver interconnector. (coating: 50 nm Pd). The palladium surface is not attack, but signs of non-plating are visible. Magn. X 15.

4.3. Auger examination

Auger spectra and depth profiles are taken on each sample. On several samples Auger analysis and depth profiling is also performed on spots which were originally covered with the adhesive tape, in order to compare a non-affected surface with an affected surface.

The main contaminants found on the silver surfaces after exposure are carbon and chlorine with smaller amounts of sulphur, oxygen and sodium. Depth profiling into the atomic oxygen attacked silver surface (fig. 3a) indicate that the sulphur and chlorine layers are very thin, but that there is a carbonaceous layer of approximately 50-100 nm thick followed by a layer which is essentially silver and oxygen of about 2 to 3 μm in thickness. This layer contains about 5% oxygen. The thickness of this layer depends on the positions of the specimens relative to the velocity vector of the spacecraft. Samples perpendicular to this vector exhibit an oxide layer in the low range while samples tested 45° to this vector have an oxide layer in the high range of the observed spread in layer thickness. Depth profiling into the reverse face of the interconnectors shows a similar film to that found on the front face with an oxide layer of about 1.5 to 2 μm thick.

The contaminants found on the gold coated samples are mainly silver, which has apparently diffused through the gold onto the free surface, with low levels of S, O, C and Si. The thickness of the silver layer found on the gold coating depends on the thickness of the underlying gold layer. Values of 20 nm and 100 nm are measured respectively for the 500 and 50 nm gold coatings. A depth profile taken from the gold surface underneath the adhesive tape shows also diffusion of silver through the gold coating, although to a lesser extent than with the exposed surface (fig. 3b, 3c). Assuming the gold layer under the adhesive tape has still its original thickness, then the gold layer in the exposed zones has decreased 26 nm in thickness.

The Auger investigations of the silicone coated silver interconnectors are as different as the SEM examinations. Surface analysis and depth profiling on specimen 6 only detected Si, C and O, while on the sample coated with DC1200 analysis in a shiny area revealed high carbon levels with Ag, S, O and Si. Apart from a very thin (5 nm) outer layer, the C signal is due to an overlap with a minor Ag line. Further profiling into this surface displays a 50 nm thin layer containing Ag, N, O and Si. A survey scan from one fo the blackened regions shows less carbon but still S, O, Ag and Si

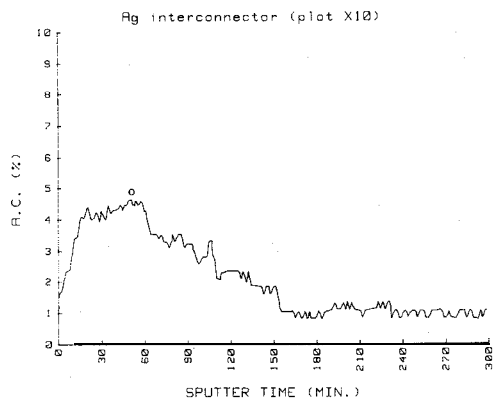


Figure 3a. Auger depth profile of oxidised silver surface. Apart from the contaminants on the surface, a silver oxide layer (oxygen content 5%) is found to a depth of approx. 1.5 μm .

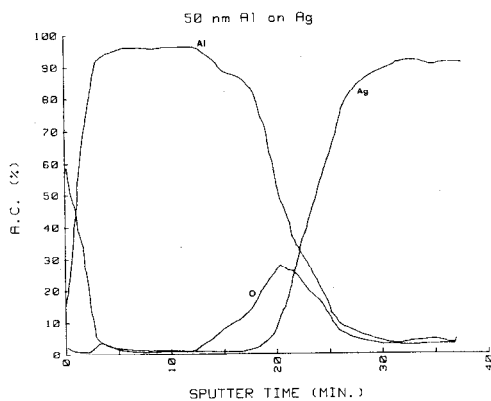


Figure 3d. Auger depth profile of exposed 50 nm Al on Ag. A small amount of Ag is found on top of the Al surface. This surface shows probably normal Al_2O_3 .

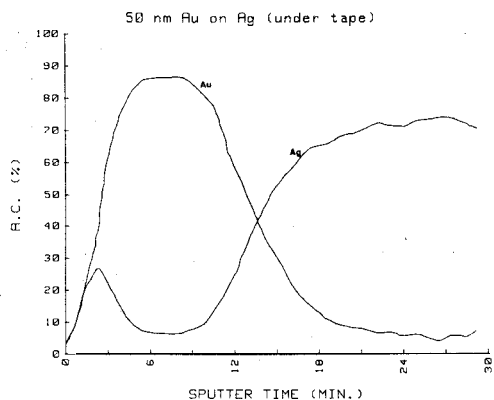


Figure 3c. Auger depth profile of unexposed 50 nm Au on Ag (same interconnector as in Fig. 2b) still a small amount of Ag is found on the Au surface.

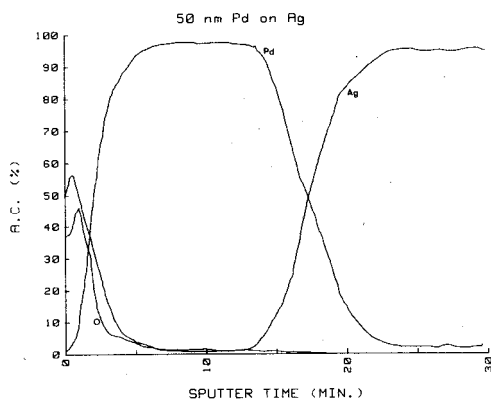


Figure 3e. Auger depth profile of an exposed 50 nm Pd layer on Ag. Some Ag diffused through the thin Pd layer is found on the surface.

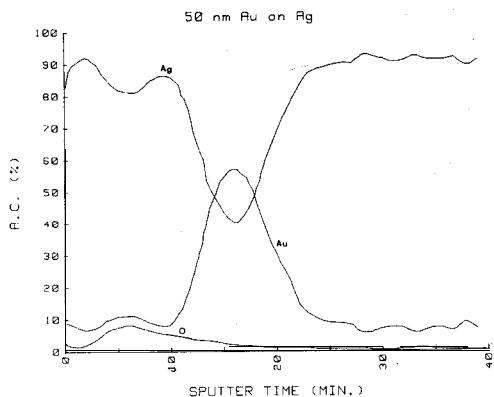


Figure 3b. Auger depth profile of an exposed 50 nm Au on Ag surface. A layer of approx. 1000 Å off Ag is found on top of the Au surface.

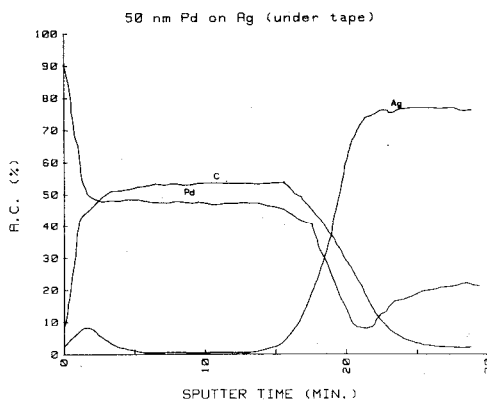


Figure 3f. Auger depth profile of an unexposed region of 50 nm Pd layer on Ag (same interconnector as in Fig. 2e).

being present. However, profiling into this surface soon removes all elements except Ag and O with the oxygen persisting for about 0.5 μm .

Surface analysis of the silver coated molybdenum is performed on the exposed areas as well as on a region underneath the adhesive tape. On the exposed areas the presence of Ag, O and a trace of S and Cl is recorded, but profiling into this surface quickly removes the traces of S and Cl while the oxygen persisted to about 1 μm below the surfaces. Besides the above mentioned elements also C and N are detected on the surface masked by the adhesive tape. After a light etch all contaminants are removed leaving pure silver.

The survey scans of both aluminium interconnectors are very identical. Apart from Al and O, Si is the only contaminant present. Depth profiling suggests a mixed layer of oxidised Si and Al of 4-5 nm thick, followed by an oxidised aluminium layer of 7-8 nm. Approaching the Al/Ag interface on the aluminium coated silver interconnector the oxygen signal rises again owing to the presence of an interfacial contaminating oxide layer, probably due to gettering of oxygen in the vacuum system during evaporation of the aluminium on the silver surface (fig. 3d).

The essential difference in surface scans between the palladium coated interconnectors is the presence of silver on the surface of the 50 nm palladium coating, which is not found on the 500 nm palladium coating. The thickness of this layer, containing both Pd and Ag is measured as 30 nm. After further profiling a pure Pd layer is encountered and no contamination is found at the Pd/Ag interface. Comparing the profile of an exposed part of the interconnector with an unexposed one (under adhesive tape) revealed a slightly thicker Pd layer in the latter case (figs. 3e, 3f). Assuming again as in the gold case, that this is the original thickness, then the exposed Pd layer has decreased 6 nm.

4.4. Microscopic examination

Transverse cross sections of some interconnectors were prepared to establish

these interconnectors. To measure this decrease crosssections through the masked of regions and the exposed regions were measured. Bare silver samples tested perpendicular to the velocity vector (sample 1) with an original thickness of 34 μm have decrease 3 μm reaching a thickness of 31 μm after atomic oxygen exposure. As already showed with the Auqer profiling, samples tested under 45⁰ to the velocity vector are attacked to a greater depth. This is also confirmed by the microscopic investigations where sample 2 exhibit a thickness decrease from 34 μm to 29.5 μm (fig. 4a).

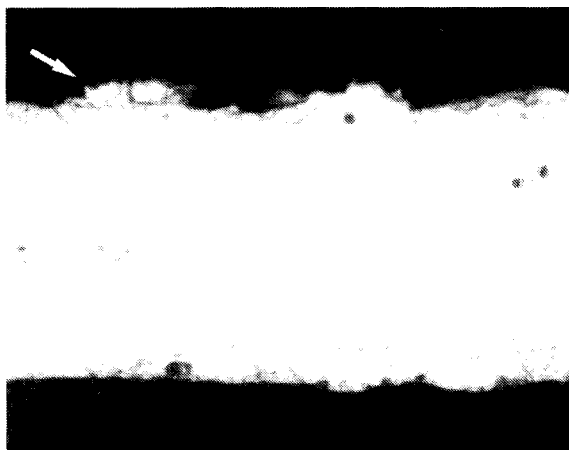


Figure 4a. Cross section through an exposed region of a silver interconnector. (45⁰ to the velocity vector). The thickness is 29.5 μm (original 34 μm). Magn. X 1500

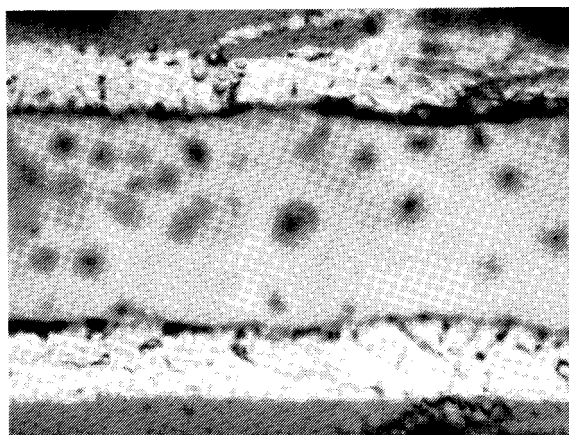
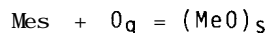


Figure 4b. Cross section through a silver coated molybdenum interconnector, showing atomic oxygen attack of the silver. No molybdenum is exposed yet.

Microscopical results of the silver plated molybdenum gives a decrease in thickness comparable to the bare silver specimens, which is not surprising since the thickness of the silver plating on the molybdenum is 5 μm (fig. 4b).

5. DISCUSSION

The bombardment of a metal surface by enough energetic oxygen atoms will always lead to the formation of an intermediate oxide layer. The direction of the oxidation reaction depends on the sign of the free energy of formation (ΔF) of the reaction. Since entropy effects are small at low temperature only the sign of the heat of formation (ΔE) of the metal oxide determines the stability of the oxide. From tabulated values of ΔE it is found that all metals except Au and Pt, exhibit negative heat of formation and thereby form stable oxides. (Silver(II)-oxide is only stable below ca. 200°C-entropy effect). The above mentioned arguments on the stability are only valid for molecular oxygen. Unlike molecular oxygen, atomic oxygen has a high positive heat of formation (heat of formation of molecular oxygen at RT per definition equals zero). The direction of the oxidation reaction:



now depends on ($\Delta E_{MeO} - \Delta E_O$), which for all metals is negative, so theoretically also Au and Pt will form oxides under atomic oxygen bombardment.

The number of atoms of a metal surface is typically ca. 10^{15} /cm². If the dose of incident atoms to the sample is lower than this (say 10^{14} atoms/cm²) then the effect of the chemical character of the incident atoms is only marginal. However, the chemical character of the atoms becomes important at high doses ($\sim 10^{15}$ atoms/cm²) where sufficient implantation has occurred to affect a change in the character of the matrix and in the matrix of the exposed surface. The Auger measurements indicate that a part of the total surface is converted to the stoichiometric oxide, since the oxygen content is ca. 5%.

In case of atomic oxygen attack in LEQ where a dose of 3×10^{20} atoms/cm² is

measured, the chemical effect of the atomic oxygen on the metal surfaces manifests itself already after about 10 seconds of exposure.

No data is available for erosion-corrosion yields of atomic oxygen on metal surfaces. As a comparison we can use sputtering yields of molecular oxygen on metal surfaces, although these are normally measured at a far more higher energy than 5 eV. (table II) In the sputtering practice a lowest energy for sputtering is normally observed. This lowest energy stems from the fact that the transfer energy of the oxygen to the metal atoms has to overcome the binding energy of the metal atoms itself. The transfer energy depends on the atoms under consideration as follows:

$$E_{\text{trans}} = (4Mm/(M+m)^2) * E_0$$

m = atomic mass of oxygen

M = atomic mass of metal

E_0 = energy of oxygen atom

The binding energies of metal atoms are typically in the range of 4-7 eV, while the mass factor is approx. 0.5. This gives a sputtering threshold of approx. 10 eV. Obviously the energy of 5 eV of the atomic oxygen is too low to have a sputtering effect on the metal surfaces, however in the case of atomic oxygen this lower energy limit is questionable, since this threshold is only valid for physical sputtering, while as argued before with oxygen, especially with the atomic variant, a large chemical effect exist. Hence, for chemical sputtering no low

TABLE II

SPUTTERING YIELDS FOR 20 KeV O ₂	
target	sputtering yield
Al	0.52 \pm 0.13
Cr	0.74 \pm 0.09
Fe	0.57 \pm 0.05
Ni	1.0 \pm 0.1
cu	3.0 \pm 0.4
Mo	0.82 \pm 0.09
Ag	9.7 \pm 0.2
Au	7.4 \pm 0.1

The sputtering yields are in atoms per ion (ref. 5 and 6).

energy limit is expected.

The parameters which mainly influence the erosion-corrosion behaviour of a metal under atomic oxygen attack are the properties of the metal oxides. The free energy of oxide formation of the metal mono-oxide can be regarded as the energy involved in breaking up the bond of the solid oxide. These energies can differ considerably from the cohesion energies of the metals themselves. Metals with a low free energy of oxide formation are expected to sputter faster (ref. 5) than the ones with a high free energy of oxide formation (compare Ag and Au with Al and Cr in table II and III).

Also transformation temperatures of the oxides like melting points, sublimation temperatures and stresses in the metal oxide layer play an important role. The large atomic oxygen effect on osmium can be explained by the low melting point of OsO_4 (assumed it is formed) of $400^\circ C$ (temperature in LEO is $+100/-100^\circ C$) but is also explained by the very low binding energy of the metal-oxide bond of ca. 1 eV and the high stresses in the oxide at low temperature, since the volume ratio of the oxide to the metal is 4.38 for osmium.

Also in the case of silver a low transformation temperature of $100^\circ C$ of the mono-oxide is found. Secondly the binding energy for silver(II)-oxide is even lower than for OsO_4 . The binding energy for Ag_2O is 0.32 eV, while the transfer energy of 5 eV O to Ag is 2.25 eV.

TABLE III

ENERGY DATA FOR SOME MATERIALS

elem	E_{coh} eV	neg. free energy of formation of O in eV	transfer energy for $5 eV O$	V_{ox}/V_m
Ag	2.94	0.32	2.25	1.61
Al	3.41	5.89	4.67	1.37
Au	3.82	-0.82	1.39	2.21
cu	3.50	1.63	3.21	1.75
Fe	4.31	2.79	3.46	1.78
mo	6.82	2.62	2.45	2.1
Ni	4.46	2.53	3.37	1.70
Os	8.15	1.01	1.43	4.38
Pd	3.90	1.19	2.27	1.59
Pt	5.86	-0.89	1.40	2.45

The other metals investigated were Au, Pd and Al. Considering that the amount of metal removal due to atomic oxygen is closely related to the binding strength of the mono-oxides, it is obvious that Pd and especially Al are less affected than Au. Palladium and its oxide are comparable with Ni and Cu and their oxides (bond strength, ratio of oxide/metal). Interpolating in table II and III between Cu and Ni gives, for $20 KeV O_2^+$, a sputtering yield for Pd of ca. 2 atoms/ion. The sputter ratio between Au and Pd then follows as 3.7. With a measured amount of gold removal during LEO exposure of 26 nm, a value of 7 nm for Pd is found, which is very close to the measured value of 6 nm found experimentally.

If a thin layer of either Au or Pd is coated onto silver, it is expected that the silver diffuses through that top layer. The driving force is the surface energy. The surface energy is related to $H_v/V_m^{2/3}$, where H_v = heat of evaporation and V_m = molar volume. This factor is low for silver compared with the ones for Au and Pd, which means that silver diffuses to the surface. This is indeed observed experimentally (see Auger results).

It can be argued that the palladium removal and especially the gold removal during LEO exposure is due to the presence of silver on both surfaces and the flaking off of the silver, removing pieces of the underlying metal. Investigation into this hypothesis can be made by comparing the cohesion energies of the different combinations. The cohesion energy of an A-B pair is given as:

$$E_{coh} = \frac{1}{2} E_{coh}^A + \frac{1}{2} E_{coh}^B + E$$

where E_{coh} = cohesion energy
 E = internal energy per atom which is $z/4 * W_{AB}$ (for solid solutions)
 W_{AB} = interaction energy between A and B
 z = coordination number

Since W_{AB} for different alloy system is in the range of 0.1 to -0.1 eV, it can be discarded in comparison to the cohesion energies. It follows that the cohesion energy of AB is the arithmetical mean of

the separate cohesion energies. If A stands for Ag and B for either Au or Pd and knowing that $E_{\text{coh}}(\text{Ag})$ is smaller than $E_{\text{coh}}(\text{Au})$ or $E_{\text{coh}}(\text{Pd})$ it is found that the bond strength between two Ag atoms is always lower than the one between the other combinations, from which it follows that bond breaking will not occur between Ag-Pd or Ag-Au or within Pd or Au itself but preferably within the silver matrix (or silver-oxide matrix).

One experimental fact is only mentioned briefly. During orbit the exposed samples undergo a thermal cycling sequence of $+100/-100^{\circ}\text{C}$. This might have a detrimental effect on some oxides. The simultaneous action of atomic oxygen attack and thermal cycling might be compared with such effects as static stress and corrosion (stress corrosion) and fatigue and corrosion (corrosion fatigue), where the result of the combined action is more than the sum of the separate effects. The pure metals are virtually unaffected by thermal cycling itself, also the effect of atomic oxygen on metals like Au, Pd and Al is in the line of expectation compared to the sputtering yields under 20 KeV O_2^+ bombardment. Following these yields, the value for silver (and osmium) has to be in the same order of magnitude. However, a dramatic effect on silver (and osmium) is observed following LEO exposure, which is believed to be the result of the combined action of atomic oxygen attack and thermal cycling. Therefore, on ground testing of materials for LEO behaviour should always incorporate both atomic oxygen attack as well as thermal cycling.

6. CONCLUSION

From experiments in LEO it is found that silver is attacked by atomic oxygen to a very large extent. Gold is also affected, although about 100 times slower than silver. The coatings which proved to be effective in protecting the underlying silver against atomic oxygen corrosion during this test were the 500 nm palladium and the silicone DC6-1104 coatings. The aluminium coated interconnector appeared to fare well with a slightly thickened oxide layer.

From these results it is clear that the use of unprotected silver, exposed during LEO, will be problematic if no reliable coating is used. Even gold and palladium layers have to be carefully optimised when as used protective coating.

7. ACKNOWLEDGEMENT

I wish to acknowledge Dr. Barry Lamb of Standard Telecommunication Laboratories, Essex, England, for performing the Auger analyses and NASA for the application of the coatings and the performing of the actual experiments.

8. REFERENCES

1. Codella P.J. The Oxidation of Silver Thin Films by Atomic Oxygen. Thesis Utah State Univ., 1977.
2. Riley J.A. and Giese C.F. Inter action of Atomic Oxygen with Various Surfaces. J. of Chem. Phys. 1970, 53, 146.
3. Wood B.J. The Rate and Mechanism of Interaction of Oxygen Atoms and Hydrogen Atoms with Silver and Gold. J. of Phys. Chem. 1971, 75, 2186.
4. Peters P.N., Linton R.C., Miller E.R. Results of the apparent atomic oxygen reactions on Ag, C and Os exposed during shuttle STS-4 orbits. Geophys. Research Letters 1983, 10, 569.
5. Vijn A.K. The Fundamental Factor determining the Sputtering Yields of Metals Bombarded with 20-KeV Oxygen Cations. J. of Mat. Sci. Letters 1985, 4, 1036.
6. Tsumoyama K., Suzuki T., Ohashi Y., Kishidaka H. Surf. Interface Anal. 1980, 2, 212.
7. Lamb B.L. and De Rooij A. Examination of Silver Solar Cell Interconnectors after Low Earth Orbit Exposure. ESTEC Working Paper EWP 1396, 1984.

DISCUSSION ON
SESSION 2: MATERIALS IN LOW EARTH ORBIT

The session covered two topics, namely the off-gassing tests/requirements and the LEO - atomic oxygen erosion.

J. Dauphin asked whether on a carbon-fibre-reinforced material the resin is attacked/eroded earlier by oxygen than the fibre itself. J. Zimcik answered that this is correct, but small particles of carbon are found on the surfaces, indicating that carbon is also affected. J. Dauphin remarked that the simultaneous existence of atomic oxygen, thermal cycles and micrometeoroids are much more serious than each environment alone.

L. Leger and M. McCargo stated that the protection layers against atomic oxygen erosion has to be applied very carefully to avoid small surface defects. It was asked whether the reduction of mechanic strength is proportional to material loss. L. Leger pointed out that (for the case of Mylar) UV effects increased strength reduction.

W. Götz wanted an explanation of the (melting-snow-like) surface condition of Kapton after atomic oxygen exposure. D. Zimcik said that it is not clear. The distance of ~1 micron between the peaks can perhaps be due to surface irregularities, cleanliness variations.

J. Dauphin made the remark that a plasma alone as atomic oxygen test medium may lead to misunderstanding. A simultaneous existence of other LEO-conditions is essential.

M. McCargo answered that a plasma test is acceptable to screen materials and can be therefore used as first approach of comparison. Furthermore it can be expected that test results obtained with oxygen atoms was different from those with oxygen ions.

J. Koch asked whether alloys between two materials with different resistance against atomic oxygen are applicable. A. de Rooij expected the sputtered layers he was speaking about behave similarly to alloys and therefore it can be expected (case Au-Ag) that the erodable material is diffusing to the surface and is there affected.

M. Hecking stated that the MAC limits are valid for 7-day missions only and should be modified for longer flights. S. Stradling confirmed.

The question whether Soviet space missions are based on the same or similar specifications as American flights could not be answered. L. Leger suggested the use of Shuttle specifications.